Nucleic Acids Research, 1994, Vol. 22, No. 4 625–631

Conformational heterogeneity in the *Salmonella typhimurium pyrC* and *pyrD* leader mRNAs produced *in vivo*

Kim I.Sørensen
Department of Biological Chemistry, Institute of Molecular Biology, University of Copenhagen, Sølvgade 83, DK-1307, Denmark

Received October 8, 1993; Revised and Accepted January 17, 1994

ABSTRACT

In *Salmonella typhimurium*, different conformations of the *pyrC* and *pyrD* leader transcripts are produced as a result of nucleotide sensitive selection of the transcriptional start site. The CTP-initiated transcripts, synthesized at high intracellular CTP/GTP pool ratios (repressing conditions), have the potential of forming a stable secondary structure at the 5′ end, thereby sequestering the site for translational initiation. At low CTP/GTP pool ratios (derepressing conditions), transcription starts 2–3 bp further downstream, resulting in transcripts with limited potential for stem-loop formation and therefore open for translational initiation. The conformation of the leader regions of wild type *pyrC* and *pyrD* mRNA has been investigated by chemical and enzymatic probing of RNA isolated from cultures grown in repressing and derepressing conditions. As controls and to obtain further information on the relation between the leader RNA conformation and the regulatory mechanism, the probing experiments also included *pyrC* and *pyrD* mRNA from mutants that contain a base substitution at a position that destabililizes the putative hairpin. In accordance with predictions based on the nucleotide sequence, the results showed that the 5′ end of *pyrC* and *pyrD* leader mRNA isolated from repressed cultures is folded into a secondary structure, whereas it is largely unstructured in mRNA isolated from derepressed cultures.

INTRODUCTION

Expression of the *pyrC* and *pyrD* gene in *Salmonella typhimurium* involves a translational control mechanism that is mediated by nucleotide sensitive selection of the transcriptional start site (1, 2). Examination of the transcripts produced *in vivo* has revealed that two lenghts of transcripts are synthesized from the *pyrC* and *pyrD* promoters. At high intracellular CTP/GTP pool ratios, transcription initiates preferentially with CTP 6 or 7 bp downstream from the pribnow box in the promoters. The leader of the resulting transcript has the potential of forming a stable secondary structure that interferes with translational initiation. At low CTP/GTP pool ratios, the RNA polymerase initiates transcription with GTP 2 or 3 bp further downstream yielding a leader transcript with limited capability to form a secondary structure (1, 2) (Figure 1). Mutants displaying high constitutive expression, due to point mutations occurring on either site of the region of dyad symmetry, have emphasized that base-pairings at the RNA level are important for repression of expression (2, 3). Additional support was provided by introducing two complementary mutations in the *pyrC* leader that individually result in high constitutive expression but when present simultanously restore wild-type regulation (1). On basis of these results and on computer calculated foldings (4), conformational heterogeneities were predicted in the *pyrC* and *pyrD* mRNA leader transcripts.

Since the regulatory model implies the formation of a secondary structure on the long C-started *pyrC* and *pyrD* leader transcript and not on the shorter G-started, it was of interest to obtain experimental evidence for the presence of such structures. In the present work, secondary structures at the 5′ end of *pyrC* and *pyrD* mRNA were identified by testing the reactivity of *in vivo* isolated leader mRNA towards enzymatic and chemical probes that specifically recognize regions on RNA located in single-stranded or double-stranded conformations. The probed nucleotides were identified by primer extension analysis of the modified mRNA.

MATERIALS AND METHODS

Bacterial strain

As host strain for the various plasmids, JL1280 (*pyrG*1611$_{leaky}$ *cdd-7 udp-2 glpT*) was used. It is a derivative of *Salmonella typhimurium* LT2 and was obtained from J.L.Ingraham. SL4213 (*metA22 metE55 galE496 rpsL120 (ilv) xyl-404 Fels2*$^-$ *H1-b nml*$^-$ *H2-enx hsdL6 hsdSA29*) was provided by B.A.D.Stocker.

Plasmids

Plasmids pJRC49, pJRC85, pMMF11 and pMMF31 all carry translational *lacZ* fusions based on the translational expression vector pRAK81 and pRAK82 (1, 3), derived from pNM481 and pNM482 (5) and a lower-copy derivative of pJRD158 (6). The

pRAK vectors contain a multiple cloning site in front of the eighth codon of *lacZ* and are devoid of most of the *lacY* gene. Plasmid pJRC49 carries a wild-type *pyrC* promoter-leader fragment (3), whereas pJRC85 contains the *pyrC* leader with a G to C mutation at a position that will destabilize the putative leader secondary structure (figure 1). Plasmid pMMF11 contains the wild-type *pyrD* promoter-leader fragment and pMMF31 carries a G to A mutation in the *pyrD* leader that will destabilize the putative hairpin at the 5′ end of *pyrD* mRNA (Figure 1). Construction of the plasmids has been described elsewhere (1, 3).

Media and growth conditions

Bacterial cultures used for isolation of RNA were grown in AB minimal medium (7), containing 0.2% of glucose and casamino acids. Supplements, were added at the following concentrations: Ampicillin, 50μg/ml; uracil, 20μg/ml; and cytidine, 40μg/ml. The *pyrG1611* allele of JL1280 encodes a partially defective CTP synthetase that results in low intracellular cytosine nucleotide pools and a high UTP pool when the strain is grown in the absence of cytidine. In the presence of exogenous cytidine, the pools are normalised (8). The strain was transformed with the appropriate plasmids and grown in derepressing (cytidine absent) or repressing (cytidine present) conditions.

DNA techniques

The procedures for plasmid isolation, restriction endonuclease digestion, ligation and transformation have been described previously (9). Plasmid constructs were initially selected in an appropriate *E.coli* strain and subsequently transformed into the restriction-negative *S.typhimurium* SL4213, before transformation to the final *S.typhimurium* host (JL1280). The chain-termination method of Sanger *et al.* (10) was used for DNA sequencing with M13 templates.

RNA extraction

Total RNA was isolated from exponentially growing cells of JL1280 containing the appropriate plasmids as described previously (1).

Enzymatic and chemical modifications of RNA

Before modification, the RNA was renatured by a 10 min. incubation at 60°C in the appropriate buffer (see below), cooled down to 25°C and placed on ice.

Chemical probing. Modification of the N-1 positions on adenine and the N-3 positions on cytosine with dimethylsulphate (DMS): In each reaction, 4 μg of renatured RNA in 200 μl 70 mM Hepes−KOH (pH 7.8), 10 mM $MgCl_2$, 270 mM KCl and 1 mM DTT was incubated at 0° C for 20 min with 1 μl of freshly made 1:1 dilution of DMS (Aldrich Chemicals Company) in ethanol. The subsequent experimental steps were carried out essentially as described by (11).

Enzymatic probing. Samples containing 4 μg renatured RNA in 20 μl 30 mM Tris−HCl (pH 7.8), 20 mM $MgCl_2$, 300 mM KCl, 1 mM DTT was used for each reaction. The protocols for digestion with RNaseT1, RNAseT2, RNaseU2 (all Sankyo), and RNaseV1 (Pharmacia) have been described in detail (11) and enzyme concentrations are written in the figure legends. Incubation time with all ribonucleases was 30 min. at 0°C.

Detection of modified positions

Analyses of mRNA 5′ends and detection of modified bases or cuts in the *pyrC* and *pyrD* transcripts were carried out by primer extension analysis as previously described (1). The primers were 5′end labeled oligonucleotides complementary to the first six codons of *pyrC* and to codons four to nine of *pyrD*. Reactions were stopped by addition of formamide-sequencing dye mix. After denaturation at 90°C for 3 min, the reverse transcripts were analysed on an 8 or 9 % polyacrylamide sequencing gels. Elongation controls (no probing) were run in parallel in order to detect nicked positions in the RNA or pausings of reverse transcriptase. Comigrating DNA sequence ladders were generated by using the same oligonucleotides as primers on M13 templates.

RESULTS

The aim of this work has been to show, by chemical and enzymatic probing, that the leader region of the the dominant *pyrC* and *pyrD* transcripts isolated from cells grown in pyrimidine repressing growth conditions is folded as predicted from the sequence (2, 3) whereas it is unstructured in the dominant transcripts obtained from derepressed cultures. Since the stem of the proposed secondary structures in the *pyrC* and *pyrD* leaders consists of C-G basepairs, the emphasis has been put on structure probings that elucidate whether these G and C residues are located in single-stranded or double-stranded regions of the leader RNA. On the basis of this, several enzymatic and chemical probes with known reactivities were chosen for the experiments. The single-strand specific probes, RNaseT1 (G-specific) and RNaseT2 (low specificity with preference to A), exhibit similar mechanisms of scission and both show a strong preference for residues located in the apex of terminal loops (11, 12, 13, 14). RNaseU2 preferentially cleaves after adenines but at physiological conditions the specificity is not absolute (A>G>>C>U) (15). DMS methylates unpaired cytosines, adenines and guanine but methylated guanines require an additional reductive step to be detected by primer extension analysis (16).

Double-stranded regions in the RNA were probed with RNaseV1 that preferentially attacks double helices with no apparent sequence specificity (11). Ribonucleases and chemical probes were added in such amounts that would give only one hit per probed region of the molecule. To help in the interpretation of the experiments, RNA specified by *pyrC* and a *pyrD* mutants with a hairpin destabilising mutation in the leaders (Figure 1), was probed along with RNA specified by wild-type leaders. The shorter G-started wild-type *pyrC* or *pyrD* leader transcripts with limited potential to form secondary structures were isolated from JL1280 harboring pJRC49 and pMMF11, respectively, grown at derepressing conditions, i.e. with no cytidine (CR) added to the medium. This mRNA will be referred to as (wt−CR) RNA. The slightly longer C-started *pyrC* and *pyrD* wild-type transcripts capable of forming secondary structures, as well as the mutated leaders without this potential were isolated from JL1280 harboring pJRC49, pMMF11, pJRC85 and pMMF31, respectively, grown with cytidine added to the medium, i.e. repressing conditions. For simplification, these two RNA types will be designated (wt+CR) and (mut+CR), respectively. The wild-type and mutant *pyrC* and *pyrD* mRNA variants were probed from the start codon, where +1 is the adenine, to the 5′ end of the transcripts.

Despite the G specifity of RNaseT1, bands indicating cleavages

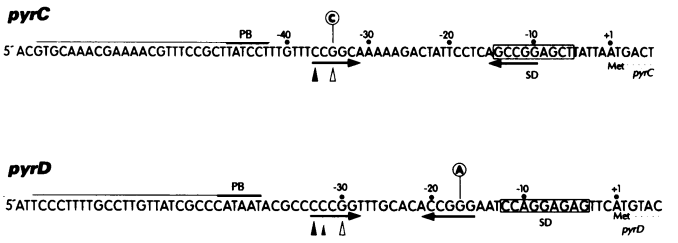

Figure 1. DNA sequence of the *Salmonella typhimurium pyrC* and *pyrD* promoter-leader. Open and closed triangles represent predominant transcriptional initiation sites in derepressing and repressing conditions respectively. Promoter regions are overlined with the pribnow boxes heavily overlined. Shine-Dalgarno regions (SD) are boxed. Regions with dyad symmetry are indicated by arrows below the DNA sequence. Nucleotides are numbered with +1 as the adenosine residue in the translational initiation codon. Circled letters indicate base substitutions in the mutant leader (mut+CR) that result in destabilisation of the putative RNA hairpin.

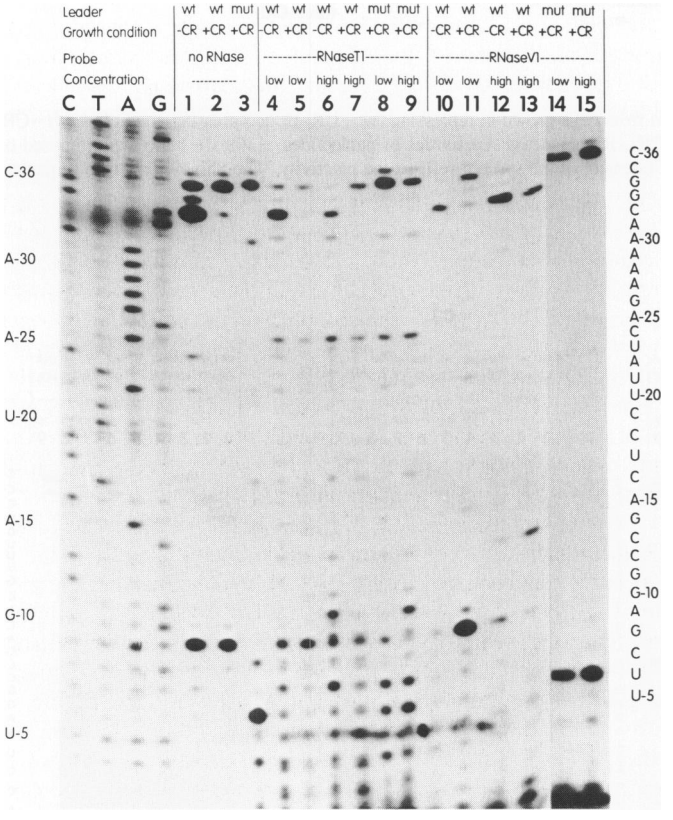

Figure 2. Reverse transcriptase results obtained with RNaseT1 and RNaseV1 treated *pyrC* mRNA: Comparison of probing data for nucleotides −36 to +1 in wild-type leader mRNA isolated in derepressing conditions (wt−CR; lanes 1, 4, 6, 10 and 12), in wild-type leader mRNA isolated in repressing conditions (wt+CR; lanes 2, 5, 7, 11 and 13), and in mutant leader mRNA isolated in repressing conditions (mut+CR; lanes 3, 8, 9, 14 and 15). Samples are: Untreated (no RNase); lanes 1−3, 0.01u (low) RNase T1; lanes 4, 5 and 8, and 0.05u (high) RNaseT1; lanes 6, 7 and 9, 0.15u (low) RNaseV1; lanes 10, 11 and 14, 0.75u (high) RNaseV1; lanes 12, 13 and 15. To facilitate direct correspondance with the mRNA sequence, the lanes representing the sequence ladder have been labeled as the complement and wild-type mRNA positions are indicated left and right to the autoradiogram. The nucleotide responsible for the stop is one postion up relative to these positions i.e. the strong cut after G-26 line up with A-25.

after U^{-26} in all *pyrD* leaders and after A^{-17} in *pyrD* (mut+CR) RNA were registered. Most likely, this implies that the reverse transcriptase has extended some transcripts partially with one nucleotide as previously observed by Egebjerg *et al.* (17). The data representing these artefact bands are not included.

To detect nicks in the RNA template or pauses of reverse transcription, elongation controls carried out on unreacted RNA were run in parallel for each experiment. Advantages and limitations of this probing approach have been discussed elsewhere (16).

For convenience, the experiments are divided into situations dealing with probing of either the *pyrC* or the *pyrD* leader mRNA's.

Structural analysis of the *pyrC* leader mRNA

Figure 2 shows the results of probing the *pyrC* leader mRNA variants with RNaseT1 and RNaseV1. Lanes 1−3 illustrate the primer extensions of non-treated RNA (elongation controls). In derepressing conditions (wt−CR, lane 1), about 70% of the *pyrC* transcripts are initiated at G^{-34} whereas transcripts isolated from repressed cultures (wt+CR, lane 2 and mut+CR, lane 3) almost exclusively are initiated at C^{-36}. A striking feature was the band at A^{-9} observed with both derepressed and repressed wild-type RNA isolated (lanes 1 and 2). Since both wild-type RNA's contained the long CTP-initiated *pyrC* transcript with the potential of hairpin formation at the 5′ end and the band was not observed with RNA from the mutant (lane 3), position A^{-9} most likely represented a partial termination site for the reverse transcriptase at the foot of the secondary structure. With mutant *pyrC* RNA (lane 3), a band was observed at position −6. This band cannot be explained in the same way as no apparent secondary structure can be formed in this region.

Probing with the single-strand specific RNaseT1 showed that the derepressed wild-type leader (wt−CR) and the leader of the mutant (mut+CR) were cleaved after the G residues located at positions −33, −26, −14, −11, and −8 (lanes 4,6 and 8,9). For G^{-14} and G^{-11} the reactivity was only clearly visible with the higher RNaseT1 concentration. However, the enhanced reactivity of G^{-11} may be due to a secondary cut (see Discussion for further details). A RNaseT1 cut at G^{-10} could only be monitored in (mut+CR) RNA (lanes 8 and 9) as a cut at this point in (wt−CR) and (wt+CR) RNA would be masked by the termination band appearing in the controls and discussed above. In contrast, the only RNaseT1 cuts observed in (wt+CR) RNA were at the positions G^{-26} and at G^{-8} just downstream from the region of dyad symmetry (lanes 5 and 7), where G^{-8} showed lower reactivity than in (wt−CR) and (mut+CR) RNA. The results of probing for double-stranded regions with RNaseV1 revealed that the only observed cuts were confined to RNA from the repressed wild-type strain (wt+CR), which was cleaved at the positions G^{-36}, G^{-35} and G^{-14} (lane 13). The latter was only apparent with the high concentration of the enzyme. The weak band at G^{-14} observed with RNA from derepressed wild-type (lane 12) probably resulted from RNaseV1 cutting of the fraction of the (wt−CR) RNA that was initiated at C^{-36} and therefore is capable of forming the hairpin. The RNA isolated from the mutant is not cleaved by RNaseV1 (lanes 14 and 15).

Other cuts were also observed, especially with high RNaseT1 and RNaseV1 concentrations. Examples were position U^{-23} and C^{-18} in all RNA types and C^{-12} in RNA from (wt−CR) and (mut+CR) and at C and U residues from C^{-7} and closer to the

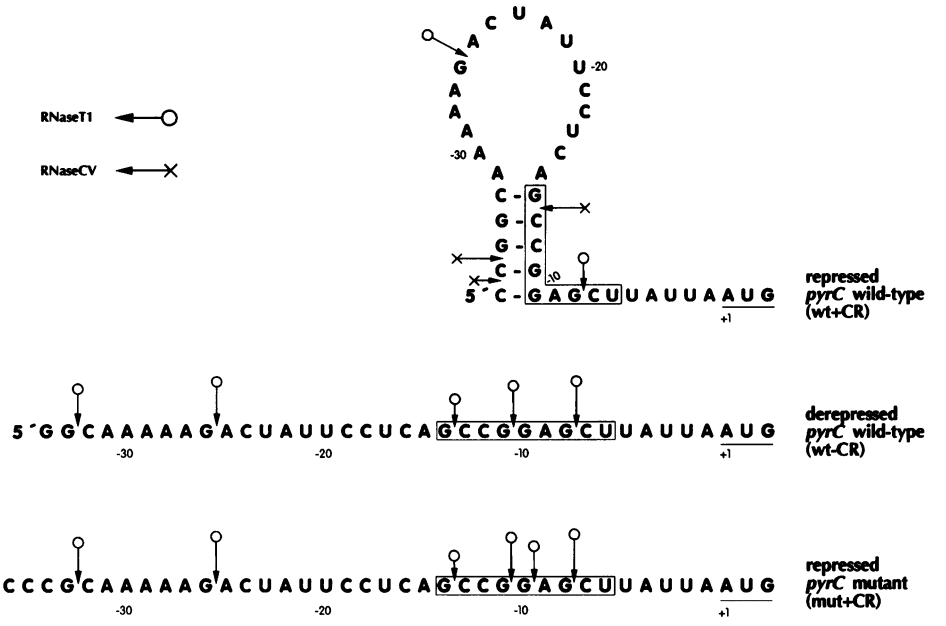

Figure 3. Putative secondary structures of wild-type *pyrC* leader mRNA isolated *in vivo* from cells grown in repressing (wt+CR) or derepressing conditions (wt−CR) or of mutant *pyrC* mRNA isolated from cells grown in repressing conditions (mut+CR). Ribonuclease reactivities of nucleotides −36 to +1 are superimposed on the structures with cuts indicated by arrows as illustrated by the legend. The length or intensity of the symbol reflects the reactivity. The Shine−Dalgarno sequences are boxed and the translational initiation codons are underlined.

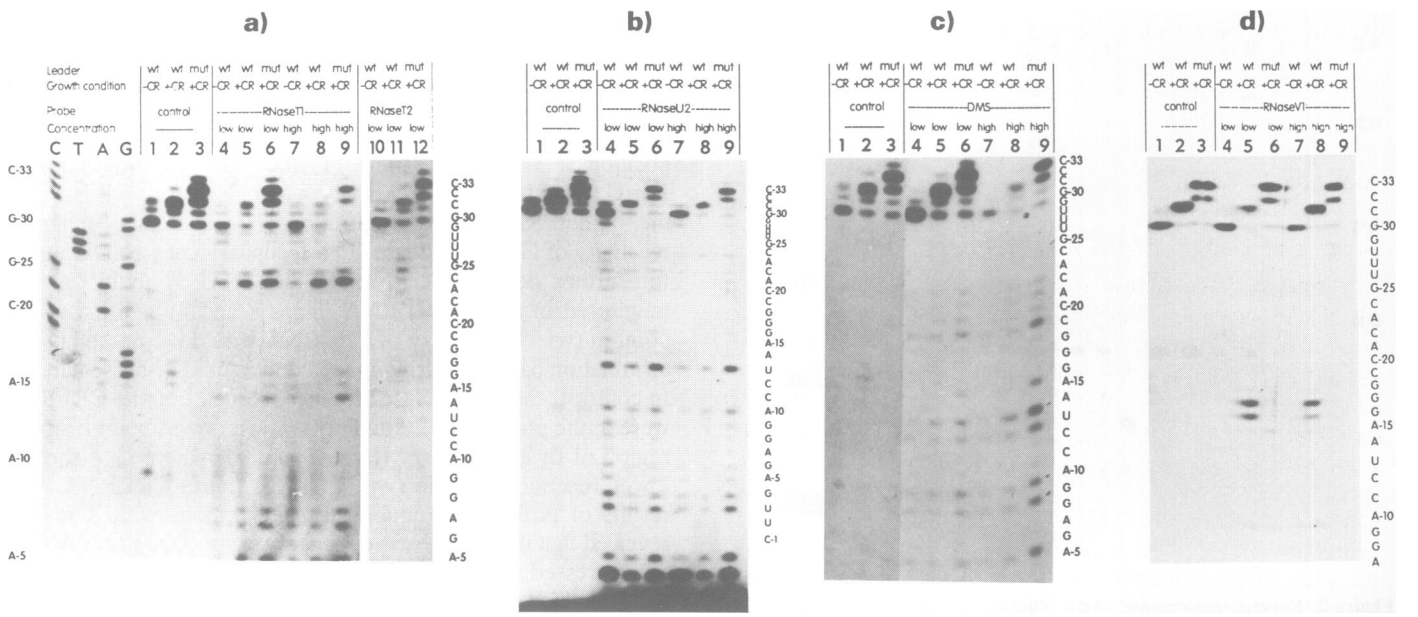

Figure 4. Reverse transcriptase results obtained with *pyrD* leader mRNA treated with RNaseT1, T2, U2, V1 and DMS: Comparison of probing data for nucleotides −33 to −1 in wild-type leader mRNA isolated in derepressing (wt−CR) and repressing (wt+CR) conditions, and in mutant leader mRNA isolated in repressing conditions (mut+CR). (**a**) RNaseT1 and T2 digestion: lanes 1, 4, 7 and 10, (wt−CR) RNA; lanes 2, 5, 8 and 11, (wt+CR) RNA; lanes 3, 6, 9 and 12, (mut+CR) RNA. Samples are: Untreated (control); lanes 1−3, 0.01u RNaseT1 (low); lanes 4−6, 0.05u (high) RNaseT1; lanes 7−9 and 0.05u (low RNaseT2); lanes 10−12. (**b**) RNaseU2 digestion: lanes 1, 4 and 7, (wt−CR) RNA; lanes 2, 5 and 8, (wt+CR) RNA; lanes 3, 6 and 9, (mut+CR) RNA. Samples are: Untreated (control); lanes 1−3, 0.05u RNaseU2 (low); lanes 4−6, and 0.25u RNaseU2 (high); lanes 7−9. (**c**) DMS modification: lanes 1, 4 and 7, (wt−CR) RNA; lanes 2, 5 and 8, (wt+CR) RNA; lanes 3, 6 and 9, (mut+CR) RNA. Samples are: Untreated (control); lanes 1−3, 1μl 1:1 (low) DMS; lanes 4−6, and 5μl 1:1 (high) DMS; lanes 7−9. (**d**) RNaseV1 digestion: lanes 1, 4 and 7, (wt−CR) RNA; lanes 2, 5 and 8, (wt+CR) RNA; lanes 3, 6 and 9, (mut+CR) RNA. Samples are: Untreated (control); lanes 1−3, 0.15u (low) RNaseV1; lanes 4−6, and 0.75u (high) RNaseV1; lanes 7−10. Wild-type mRNA positions are indicated right to the autoradiograms. The nucleotide responsible for the stop is one postion up relative to these positions i.e. the strong RNaseT1 cut after G-25 line up with C-24 (figure 4a).

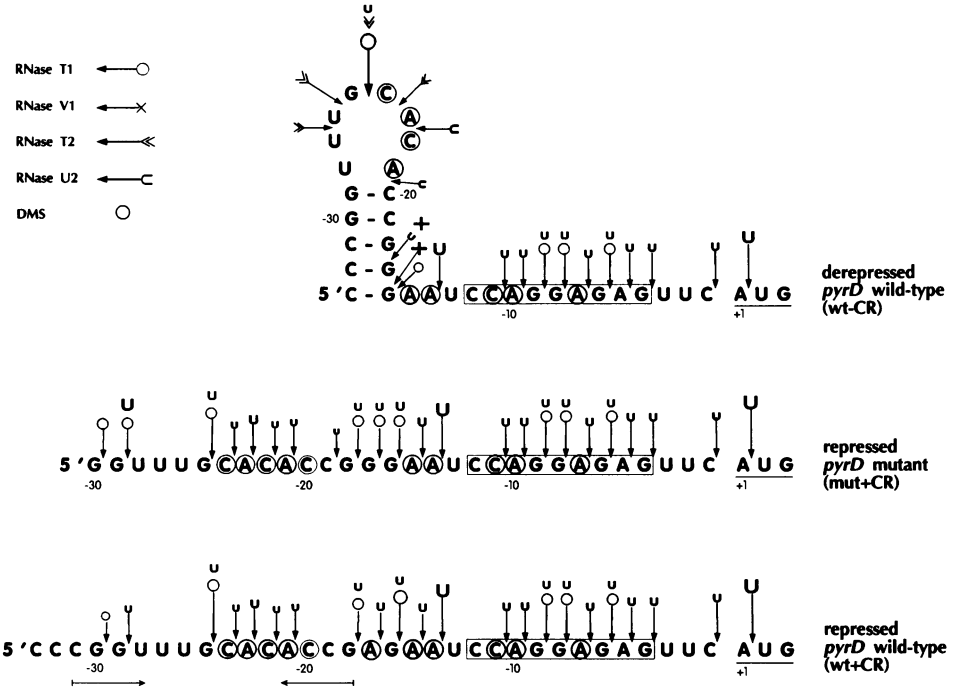

Figure 5. Putative secondary structures of wild-type *pyrD* leader mRNA isolated *in vivo* from cells grown in repressing (wt+CR) or derepressing conditions (wt−CR) or of mutant *pyrD* mRNA isolated from cells grown in repressing conditions (mut+CR). Reactivities of nucleotides −33 to +1 are superimposed on the structures with RNase cuts indicated by arrows and DMS modified residues encircled as illustrated by the legend. The length or intensity of the symbol reflects the reactivity. The Shine−Dalgarno sequences are boxed and the translational initiation codons are underlined. Arrows below the mutant *pyrD* RNA sequence indicate a small region of dyad symmetry explained in Discussion.

primer. Since these cuts occured at C and U residues located in single-stranded regions (not at C^{-12} in (wt+CR) RNA), they most likely were caused by a weak contamination with the single-strand specific RNaseA.

The data are superimposed on the putative *pyrC* leader mRNA structures in figure 3.

Structural analysis of the *pyrD* leader mRNA

The reverse transcriptase results obtained with probed *pyrD* mRNA leaders are presented in figure 4. Elongation controls have been included for experiments that were conducted separately and are presented in lanes 1−3 of the figure. They showed that more than 80% of wild-type *pyrD* transcripts from the derepressed culture (wt−CR) were initiated with GTP at position −30, and that approximately 70% of the transcripts were initiated with the CTP at positions −33 and −32 in the repressed cultures (wt+CR) and (mut+CR). With (wt+CR) RNA, the extented fragments corresponding to positions C^{-33} and C^{-32} were collapsed due to base-pairings of the nucleotides in the region of dyad symmetry. The weak bands at residues A^{-15}, G^{-16}, G^{-17} and G^{-18} in the elongation controls of (wt+CR) RNA most likely represented prematurely terminated extension products caused by the secondary structure on the RNA template.

Because *pyrD* mRNA under all growth conditions appeared to be a mixture of transcripts with different potentials for secondary structure formation at the 5′ end, the structural analyses were carried out with several different probes to facilitate the interpretation.

The most striking differences in reactivity pattern between the various *pyrD* leaders were registered in the regions $G^{-30}G^{-29}$, $U^{-27}UGC^{-24}$ and $C^{-20}CGGG^{-16}$. The guanosines at −30 and −29 were cleaved by RNaseT1 and the guanosine at −29 by RNaseU2 mainly in (wt−CR) RNA but showed almost no reactivity in (wt+CR) RNA (figure 4a and b). Strikingly, the residues in the $U^{-27}UGC^{-24}$ region are only reactive towards RNAseT2 in (wt+CR) RNA with the major cut occuring between U^{-26} and G^{-25} (figure 4a, lane 11). Simultanously, strong RNaseT1 cuts were observed after G^{-25} and with higher reactivity in (wt+CR) RNA relative to (wt−CR) RNA (figure 4a). In the region encompassing $C^{-20}CGGG^{-16}$, the C^{-20} residue was marginally reactive towards DMS in (wt−CR) and (mut+CR) RNA (figure 4c) and C^{-19} was cleaved by RNaseU2 only in (wt−CR) RNA (figure 4b). RNaseT1 and RNaseU2 cuts were registered after G^{-18}, G^{-17} and G^{-16} in (wt−CR) RNA and after G^{-18} and G^{-16} in (mut+CR) RNA (figure 4a and 4b). The A^{-17} position in (mut+CR) RNA was cleaved by RNaseU2 and methylated by DMS (figure 4b and 4c). In the same region, (wt+CR) RNA was only cleaved significantly by RNaseT1 after G^{-16} (figure 4a). In contrast, the guanosines at −18 and −17 within this region of (wt+CR) RNA are fully accessible to RNaseV1 whereas RNA from (wt−CR) and (mut+CR) showed no reacitivity towards RNaseV1 (figure 4d).

The remaining residues exhibited a similar reactivity pattern in all the *pyrD* leaders indicating they are located in regions with similar conformation. The accumulated data are superimposed on the putative *pyrD* leader mRNA structures (figure 5).

DISCUSSION

This paper presents the results of probing the various *pyrC* and *pyrD* leader transcripts extracted from exponentially growing

cells. Although a complete structural analysis of the *pyrC* and *pyrD* leader transcripts was beyond the scope of this work, the data obtained provide supporting evidence for the existence of different leader conformations as proposed in the regulatory model for *pyrC* and *pyrD* expression (1, 2). Inspection of the transcript bands originating from primer extension analysis of the non-probed RNA (elongation controls) gives an indication of the different structural forms of the leader transcripts. Primer extension of *pyrC* and *pyrD* mRNA with potential to form secondary structure (wt+CR) results in the occurence of 'termination bands' at positions corresponding to the foot of the hairpin or resulted in a severe compression of the long cDNA transcripts. These effects are relieved by mutations that destabilize the secondary structure.

More direct evidence for the existence of two different conformations in the *pyrC* leader is obtained from the RNaseT1 and RNaseV1 probings of *pyrC* mRNA, as summarized in figure 3. The occurrence of RNaseT1 cuts after the G residues at −33, −26, −14, −11 and −8 in the leader of the short G-started transcript (wt−CR) and the absolute absence of double-strand specific RNaseV1 cuts indicate that this leader mRNA most likely is single-stranded. The long C-started wild-type transcript isolated from the repressed culture (wt+CR), on the other hand, is not cleaved by RNaseT1 at any of the G-residues within the region of dyad symmetry, i.e. positions −36 to −32 and −14 to −10, but only in the loop region (G^{-26}) and outside the symmetry (G^{-8}). The weaker reactivity of the G^{-8} residue in the (wt+CR) leader probably reflects that the bulky RNaseT1 enzyme is sterically hindered by the proximity of the hairpin. Furthermore, the residues at −36, −35 and −14 within the dyad symmetry exhibit reactivity towards RNaseV1 indicating that these nucleotides are involved in formation of a double-stranded helix. The importance of base-pairings in this region for secondary structure formation is further demonstrated by the probing results obtained with RNA from the *pyrC* mutant carrying a C to G mutation that interrupts the dyad symmetry.

The cleavage pattern of the mutant mRNA is similar to what was obtained with the shorter G-started wild-type transcript supporting that the presence of this mutation in the long C-started transcript results in a conformational change from structured in the wild-type transcript to unstructured in the mutant mRNA. The increased reactivity of G^{-11} observed at the high RNaseT1 concentration in (wt−CR) and (mut+CR) RNA is probably a secondary effect. A primary cut at G^{-10}might render G^{-11} more flexible, whereas the same residue in (wt+CR) RNA is still base-paired.

The conformational heterogeneity in the wild-type *pyrD* mRNA leaders are indicated by several lines of evidences as summarized in figure 5. The nucleotides comprising the region for the postulated hairpin (C^{-33}–G^{-16}) in (wt+CR) RNA show a different pattern of reactivity than the corresponding residues in (wt−CR) RNA (G^{-30}–G^{-16}). In the dyad symmetry region of (wt+CR) RNA (C^{-33}–G^{-29} and C^{-20}–G^{-16}), the absence or low reactivity of the residues towards the single-strand specific probes (RNaseT1, RNaseT2, RNaseU2 and DMS) and the simultanous presence of RNaseV1 cuts after G^{-18} and G^{-17} indicate that this region has a helical conformation defining the stem of the structure. The weak reactivity towards single-strand specific probes, observed at some of the nucleotides within the dyad symmetry region of (wt+CR) RNA, most likely originates from cleavage or modification of the small fraction of G^{-30} started transcripts present in (wt+CR) mRNA.

In contrast, residues G^{-30} to G^{-29} and C^{-20} to G^{-16} in (wt−CR) RNA appear to reside in single-stranded regions, as indicated by the non-reactivity of these nucleotides towards RNaseV1 and their reactivity towards the single-strand specific probes.

Furthermore, nucleotides in the U^{-28}UUGCAC^{-22} region, corresponding to the loop of the hairpin, are reactive towards single-strand specific probes in (wt−CR) RNA and (wt+CR) RNA indicating that this region is single-stranded in both leader transcripts. Interestingly, the G^{-25} residue in (wt+CR) mRNA shows a markedly strong reactivity towards RNaseT1 and the residues within the U^{-27}UGC^{-24} region are highly reactive towards RNaseT2. In fact, RNaseT2 only cleaves within this region in (wt+CR) RNA, not in RNA from (wt−CR) and (mut+CR). According to the known preferences of RNaseT1 and RNaseT2 (13, 14), these results seem to indicate that the U^{-27}UGC^{-24} region in (wt+CR) RNA is located in the apex of a terminal hairpin loop, which is in full agreement with the predicted conformation of this leader mRNA. The *pyrD* hairpin is more compact than its *pyrC* equilvalent and has the smaller loopsize characteristic of hairpin loops (18).

The slightly weaker reactivity of A^{-21} and A^{-15} in (wt+CR) RNA towards RNaseU2 might indicate that the proximity of these residues to the stem of the hairpin represent a minor handicap for the bulkier RNase to cleave the RNA at these points. The nucleotides in the region from A^{-15} to A^{+1} of both (wt−CR) and (wt+CR) RNA are cleaved and modified to almost the same extent by RNaseT1, RNaseU2 and DMS indicating that this region is unstructured in both transcript variants.

Probing of the mutant leader mRNA (mut+CR) shows a reactivity pattern similar to what is observed with the G-initiated wild-type leader transcript indicating an open leader conformation consistent with the postulated structure. Similar to the *pyrC* situation, this illustrates that a mutation resulting in a decreased regulatory control also destabilises the secondary structure. It should be mentioned that the G residues at −30 and −29 and the C's residues at −20 and −19 tend to be slightly less reactive towards the single-strand specific probes in the RNA isolated from the mutant (mut+CR) than in the (wt−CR) RNA. The C-TP-started transcript from the mutant has a short region of partial dyad symmetry (illustrated with arrows below the RNA in figure 5) allowing the leader to form a rather unstable hairpin with a 3 bp long stem. A fraction of the transcripts may therefore form a weak hairpin in the 5′ end making the paired nucleotides less accessible. The low level of pyrimidine regulation of *pyrD* expression observed with this mutant (2) supports this observation.

ACKNOWLEDGEMENTS

I would like to thank Jan Christiansen and Roger A.Garrett for numerous helpfull discussions and for providing some of the ribonucleases used in this work. I also want to thank Jan Neuhard for critical comments and for reading the manuscript and Rodney A.Kelln for kindly providing plasmid pMMF11 and pMMF31. This investigation was supported by grants from the Danish Natural Science Council and the Danish Center for Microbiology.

REFERENCES

1. Sørensen, K. I., and Neuhard, J. (1991) *Mol. Gen. Genet.* 225, 249–256
2. Frick, M. M. , Neuhard, J. and Kelln, R.A. (1990) *Eur. J. Biochem.* 194, 573–578

3. Kelln, R. A. and Neuhard, J. (1988) *Mol. Gen. Genet.* 212, 287–294.
4. Zuker, M. and Stiegler. P. (1981) *Nucleic Acids Res.* 9, 133–148
5. Minton, N. P. (1984) *Gene* 31, 269–273.
6. Davidson, J., Heusterspreute, M., Merchez, M., and Brunel, F. (1984) *Gene* 28, 311–318.
7. Clark, D. J., and Maaløe, O. (1967) *J. Mol. Biol.* 23, 99–112
8. Lu, C-D, Kilstrup, M., Neuhard, J., and Abdelal, A. (1989) *J. Bacteriol.* 171, 5436–5442.
9. Neuhard, J., Stauning, E., and Kelln, R. A. (1985) *Eur. J. Biochem.* 146, 597–603.
10. Sanger, F., Nicklen, S., and Coulson, A. R. (1977) *Proc. Natl. Acad. Sci.* 74, 5463–5467.
11. Christiansen, J., Egebjerg, J., Larsen, N., and Garrett, R.A. (1990) In ribosomes and protein synthesis: A practical approach (Spedding, G., ed.), pp. 229–252, IRL Press, Oxford.
12. Warrington, R.C. (1974) *Biochim. Biophys. Acta* 353, 63–68
13. Heinemann, U. and Saenger, W. (1982) *Nature*, 299, 27
14. Uchida, T. and Egami, F. (1967) In: Methods in Enzymology, Grossman, L. and Moldave, K. Eds Acad. Press, N. Y., Vol. XII, pp. 228–247
15. Uchida, T., Arima, T. and Egami, F. (1970) *J. Biochem.* 67, 91–102
16. Ehresmann, C., Baudin, F., Mougel, M., Romby, P., Ebel, J. P. and Ehresmann, B. (1987) *Nucleic Acids Res.* 15, 9109–9128.
17. Egebjerg, J., Leffers, H., Christensen, A., Andersen, H., Garrett, R. A. (1987) *J. Mol. Biol.* 196, 125–136
18. Zuker, M. (1989) In : Methods in Enzymology, Dahlberg, J. E. and Abelson, J. N: eds. Acad. Press, San Diego., Vol. 180, pp. 262–288.